Journal of the Serbian Chemical Society
JSCS@tmf.bg.ac.yu • www.shd.org.rs/JSCS

J. Serb. Chem. Soc. 74 (1) 1–13 (2009)
JSCS–3803

UDC 578.7:616.988.7:598.2
Original scientific paper

Some novel insights into the binding of oseltamivir and zanamivir to H5N1 and N9 influenza virus neuraminidases: a homology modeling and flexible docking study

MARIJA L. MIHAJLOVIĆ[1,2#] and PETAR M. MITRAŠINOVIĆ[2*#]

[1]*Faculty of Physical Chemistry, University of Belgrade, Studentski trg 12–16, 11000 Belgrade and* [2]*Institute for Multidisciplinary Research, Kneza Višeslava 1, 11030 Belgrade, Serbia*

(Received 2 April, revised 21 October 2008)

Abstract: In the context of the recent pandemic threat by the worldwide spread of H5N1 avian influenza, novel insights into the mechanism of ligand binding and interaction between various inhibitors (zanamivir – ZMV, oseltamivir – OTV, 2,3-didehydro-2-deoxy-*N*-acetylneuraminic acid – DANA, peramivir – PMV) and neuraminidases (NA) are of vital importance for the structure-based design of new anti-viral drugs. To address this issue, three-dimensional models of H5N1-NA and N9-NA were generated by homology modeling. Traditional residues within the active site throughout the family of NA protein structures were found to be highly conserved in H5N1-NA. A subtle variation between lipophilic and hydrophilic environments in H5N1-NA with respect to N9-NA was observed, thus shedding more light on the high resistance of some H5N1 strains to various NA inhibitors. Based on these models, an ArgusLab4/AScore flexible docking study was performed. The conformational differences between OTV bound to H5N1-NA and OTV bound to N9-NA were structurally identified and quantified. A slight difference of less than 1 kcal mol^{-1} between the OTV-N9 and OTV-N1 binding free energies is in agreement with the experimentally predicted free energy difference. The conformational differences between ZMV and OTV bound to either H5N1-NA or N9-NA were structurally identified. The binding free energies of the ZMV complexes, being slightly higher than those of OTV, are not in agreement with what was previously proposed using homology modeling. The differences between ZMV and OTV are suggested to be ascribed to the presence/absence of Asn166 in the active cavity of ZMV/OTV in H5N1-NA, and to the presence/absence of Ser165 in the binding site of ZMV/OTV in N9-NA. The charge distribution was evaluated using the semi-empirical AM1 method. The trends of the AM1 charges of the ZMV and OTV side chains in the complexes deviate from those previously reported.

Keywords: H5N1 avian influenza virus neuraminidase; homology modeling; zanamivir; oseltamivir; Argus Lab 4.0 docking.

* Corresponding author. E-mail: petar.mitrasinovic@cms.bg.ac.yu
# Serbian Chemical Society member.

doi: 10.2298/JSC0901001M

INTRODUCTION

Due to the recent pandemic threat by the worldwide spread of H5N1 avian influenza, the World Health Organization has shown its profound concern regarding the possibility of an imminent spread of the virus among humans. Reports about the resistance of the virus to two approved anti-influenza drugs (OTV – Tamiflu, ZMV – Relenza, Fig. 1), which target the neuraminidase (NA) enzymes of the virus, as well as the lack of an adequate vaccine have raised the urgent question of developing new anti-viral drugs.[1] Even though influenza virus NA has hitherto been structurally well studied, the structure of H5N1-NA offers new opportunities for drug design.[2]

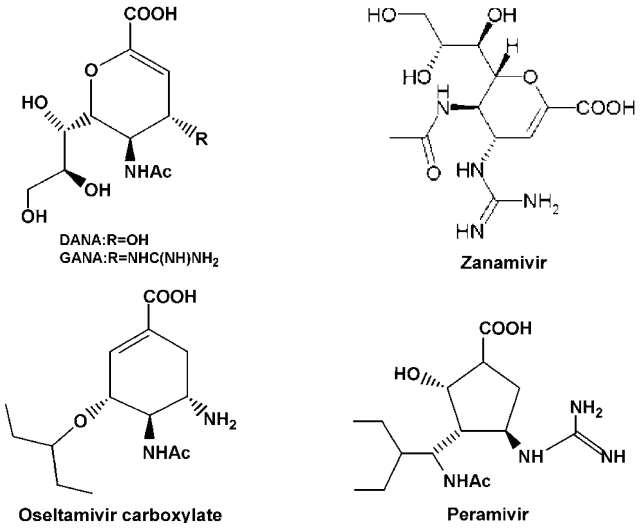

Fig. 1. The chemical structures of DANA, zanamivir, oseltamivir and peramivir.

Computational methods, such as homology modeling and flexible docking, have been identified as viable partner to experiment in the structure-based design of more potent H5N1-NA inhibitors.[3–6] Due to some controversy between the experimentally and computationally predicted susceptibilities of OTV to N1 and N9,[7] a deeper understanding of the mechanism of ligand binding and interaction between commercial drugs and NAs is currently indispensable. To place the controversy on a more rational ground, NA structural models of a quite satisfactory stereochemical quality have been herein employed to provide several novel insights into the binding of ZMV and OTV to H5N1-NA and N9-NA.

EXPERIMENTAL

Homology modeling of H5N1-NA and N9-NA

Comparative modeling is a quite useful means of predicting unknown 3D protein structures by both starting from a known primary structure and relying on known 3D structures of homologous proteins. Sequentially related proteins are assumed to adopt similar conforma

tions, atomic positions in homologous regions are borrowed from known protein structures, while non-homologous portions are predicted in various ways, including potential energy minimization, molecular dynamics and simulated annealing. Two most convenient criteria for similarity are: a) an identity of at least 25 % for a sequence size > 100 amino acids and b) an expectation (E) < 10^{-4}, which gives the likelihood that similarities are due to chance. The NA protein, containing 449 amino acids from the highly pathogenic chicken H5N1 A viruses isolated during the 2003–2004 influenza outbreaks in Japan (Accession No. Q5H895) was chosen to be modeled.[8] The sequence of N9-NA (Accession No. Q84070), which contains 470 amino acids, was also selected for modeling.[9] Swiss-Model, an automated comparative modeling approach accessible *via* the ExPASy web server, was employed for the prediction of 3D NA structures.[10] The H5N1-NA model (Fig. 2) was based on the template with a resolution of 2.5 Å (PDB ID: 2htyG),[2] while the N9-NA model was based on the template crystal structure having a 1.4 Å resolution (PDB ID: 1f8dA).[11] The two crystal structures were identified as the best templates in terms of both sequence identity and E value. To drive the generated coordinates toward optimal geometry, energy minimization on the constructed structures was performed using the Newton subroutine within the Tinker suite of programs, known as the Software Tools for Molecular Design running under the Windows operating system.[12] Running the modeling tools was facilitated by Force Field Explorer 4.2, a graphical user interface to Tinker.[13] The Amber force field parameter set (amber99.prm), as implemented in the Tinker distribution, was used.[14] The Newton algorithm is usually the best choice for minimizations to the 0.01 to 0.000001 kcal mol^{-1} $Å^{-1}$ level of root-mean-square (rms) gradient convergence. The 0.0001 criterion was chosen in the computations. To evaluate the stereochemical quality of the optimized protein structures by considering their G-factors, the final structures were analyzed by the Procheck program.[15,16] The G-factor provides a measure of how "normal", or alternatively how "unusual", a given stereochemical property is. In Procheck, both various combinations of torsion angles and covalent geometry are computed taking into account the main-chain bond lengths and the main-chain bond angles. The G-factor is a score based on the observed

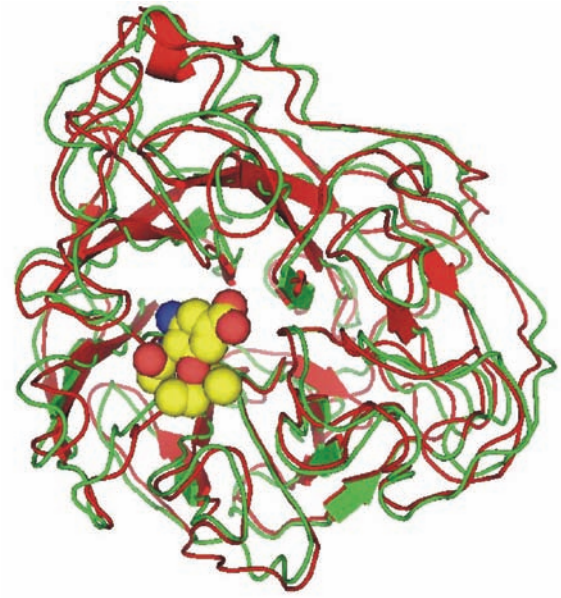

Fig. 2. A cartoon representation of the 3D-structural model of H5N1 superimposed on the 2htyG template and complexed with oseltamivir. The model is colored in red, the template is given in green, and the ligand is rendered in space-filling representation.

distributions of these stereochemical parameters. When applied to a given residue, a low *G*-factor indicates that the property corresponds to a low-probability conformation. For example, residues falling in the disallowed regions of the Ramachandran plot will have a low (or very negative) *G*-factor. Ideally, the scores should be above –0.5. Values below –1.0 may need investigation. For the H5N1-NA and N9-NA optimized models, the estimated G factors were –0.5 and –0.48, respectively. Figures shown in this article were generated by PyMol.[17] Figure 2 shows that the generated model and the template structure of H5N1-NA overlap nicely to a great extent, except in the loop regions due to the sequence alignment.

ArgusLab4/AScore/ShapeDock flexible docking

The docking problem is conceivable as a complicated optimization or an exhaustive search problem involving many degrees of freedom. Hence, the development of efficient docking algorithms would be of vital importance for the design of new drugs. The ultimate goal is to find the optimal ligand/protein configurations and accurately as well as consistently predict their binding free energy without relying on formal statistical mechanics approaches. To computationally accomplish the key objective within a reasonable time framework, an empirical scoring function (AScore) and a docking engine (ShapeDock) were developed in the ArgusLab 4.0 program.[18]

The AScore is based on the deconvolution of the total protein–ligand binding free energy into several distinct components:

$$\Delta G_{\text{binding}} = \Delta G_{\text{vdW}} + \Delta G_{\text{hydrophobic}} + \Delta G_{\text{H-bond}} + \Delta G_{\text{H-bond(chg)}} + \Delta G_{\text{deformation}} + \Delta G_0 \quad (1)$$

The dissected terms account for the van der Waals interaction between the ligand and the protein, the hydrophobic effect, the hydrogen bonding between the ligand and the protein, the hydrogen bonding involving charged donor and/or acceptor groups, the deformation effect, and the effects of the translational and rotational entropy loss in the binding process, respectively. The intra-ligand van der Waals energy is also included in the overall vdW term. These contributions can be conveniently written as the following products: $\Delta G_{\text{vdW}} = C_{\text{vdW}} \times vdW$, $\Delta G_{\text{hydrophobic}} = C_{\text{hydrophobic}} \times HP$, $\Delta G_{\text{H-bond}} = C_{\text{H-bond}} \times HB$, $\Delta G_{\text{H-bond(chg)}} = C_{\text{H-bond(chg)}} \times HB(\text{chg})$, $\Delta G_{\text{deformation}} = C_{\text{rotor}} \times RT$ and $\Delta G_0 = C_{\text{regression}}$. Each of the contributions possesses a specific regression coefficient multiplying a term that has a clear physical meaning. Investigating the regression coefficients enables more profound insights into the receptor–ligand binding process.

The ShapeDock docking engine approximates a complicated search problem. Flexible ligand docking is available by describing the ligand as a torsion tree. Groups of bonded atoms that do not have rotatable bonds are nodes, while torsions are connections between the nodes. The topology of a torsion tree is a determinative factor influencing efficient docking. A balanced tree with a large central node is presumably the favorite case. Two grids, overlaying the binding site, distinguish grid points with respect to the free volume of the binding site. A fine grid is used to examine whether atoms of a pose fragment are inside or outside the binding site, while a coarse grid is used to establish the search points inside the binding site. A set of energetically favorable rotations is generated by placing the root node of a ligand on a search point in the binding site. The torsion search of poses is defined by constructing torsions in breadth-first order for each rotation. Of the surviving poses candidates, the *N*-lowest energy poses (*N* usually 50–150) makes the final set of poses undergoing coarse minimization, re-clustering and ranking. The AScore/ShapeDock docking protocol is fast, reproducible, and formally explores all energy minima. To illustrate this standpoint, typical ShapeDock times for ligands with 10–15 torsions are shorter than 30 s on a 2.4 GHz Pentium computer.

RESULTS AND DISCUSSION

Based on different antigenic properties of various glycoprotein molecules, influenza type A viruses are classified into the following subtypes: 16 for haemagglutinin (H1–H16) and 9 for neuraminidase (N1–N9). Two phylogenetically distinct groups, group 1 (N1, N4, N5, N8) and group 2 (N2, N3, N6, N7, N9), contain N1 and N2 NAs of viruses that currently circulate in humans. One of such viruses is the H5N1 avian influenza, which is threatening a new pandemic.[2] There have also been indications that inhibitor structure/activity relationships do not apply across subtypes.[19] To learn more on the subtle differences between the active cavities of two subtypes, it is necessary to explore hydrophobic effects, as they are a key factor underlying drug design.

Even though well-established residues in the active sites are highly conserved across influenza A NA subtypes, NA inhibitors tend to show different affinities for two influenza subtypes, such as N1 and N9. The different activities are presumably due to a small, but significant, difference between two lipophilic environments. Thus, the lipophilic and hydrophilic surfaces of H5N1-NA and N9-NA are shown in Fig. 3. Note a subtle variation between the lipophilic and hydrophilic environments in H5N1-NA with respect to N9-NA. A partially lipophilic pocket containing Ala261 and Tyr262 in H5N1-NA is lined up by two hydrophilic residues, Asn265 and Asn266, in N9-NA. A partially hydrophilic pocket containing Ser165 and Asn166 in H5N1-NA is lined up with two lipophilic residues, Ala166 and Thr167, in N9-NA. The particular mutations within the H5N1-NA protein structure might be correlated with the high resistance to the existing NA inhibitors.[6] When inhibitor binding depends on either interactions with non-essential active-site amino acids or active-site amino-acid reorientation, the possibility of genomic H5N1 mutants escaping might increase.

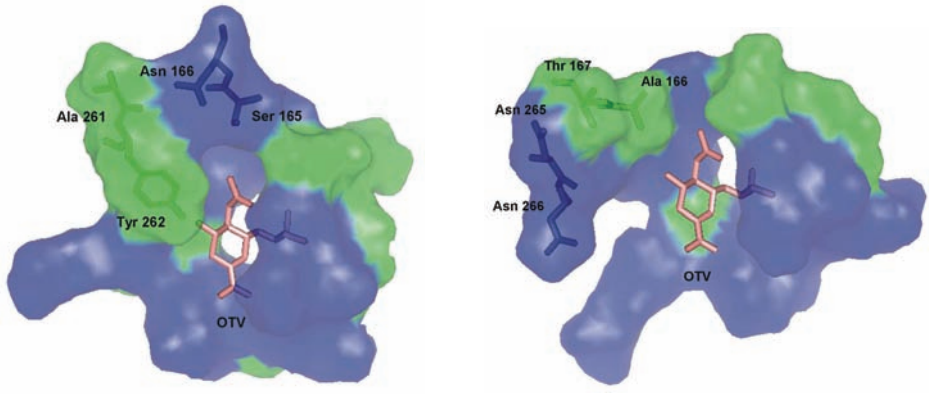

(a) (b)

Fig. 3. Lipophilic (green) and hydrophilic (blue) environments (residues) near or in the active site of H5N1-NA (a) and N9-NA (b).

A hydrophobic difference in the binding region of the glycerol side chain has been proven to be particularly sensitive.[20] To fundamentally understand the inhibitory activity of ligands such as ZMV and DANA, it is important to focus on the lipophilic and hydrophilic interactions between their glycerol side chains and the active pockets. The glycerol side chain of both ZMV and DANA has three hydrophilic hydroxyl groups and lipophilic carbons (C8 and C9) and can, therefore, be viewed as a partially lipophilic group. The lipophilic pocket formed by Arg144, Glu197 and Ala166 in the complex of N9-NA with ZMV and DANA is not present in the complex of H5N1-NA with these two ligands.[6] In ZMV/DANA-H5N1--NA, the glycerol group is tightly bound to Ser165 and Glu196 by the formation of 4 hydrogen bonds, without being able to adapt itself to the changed lipophilic environment.[6] In this respect, OTV, having an –O–R group instead of the glycerol side chain, is quite a different inhibitor than either ZMV or DANA (Fig. 1). The binding interactions of oseltamivir with the residues in the active site of H5N1-NA and N9-NA are schematically shown in Fig. 4. It is well established that two or three Arg residues surrounding the carboxylic group of a ligand, which makes strong electrostatic interactions with these particular Arg residues, are the predominant factor for orienting and stabilizing various inhibitors.[21,22] In OTV/N9-NA, there is only Arg37 in the immediate vicinity of the $–COO^-$ group, which makes an electrostatic interaction with the particular Arg residue. In contrast to this, note the two Arg residues (Arg36 and Arg74), in addition to Glu37, in the immediate vicinity of the carboxylic group, which makes strong charge––charge interactions with each of the particular residues in OTV/H5N1-NA. Therefore, the more stabilizing effect of the H5N1-NA binding site relative to the

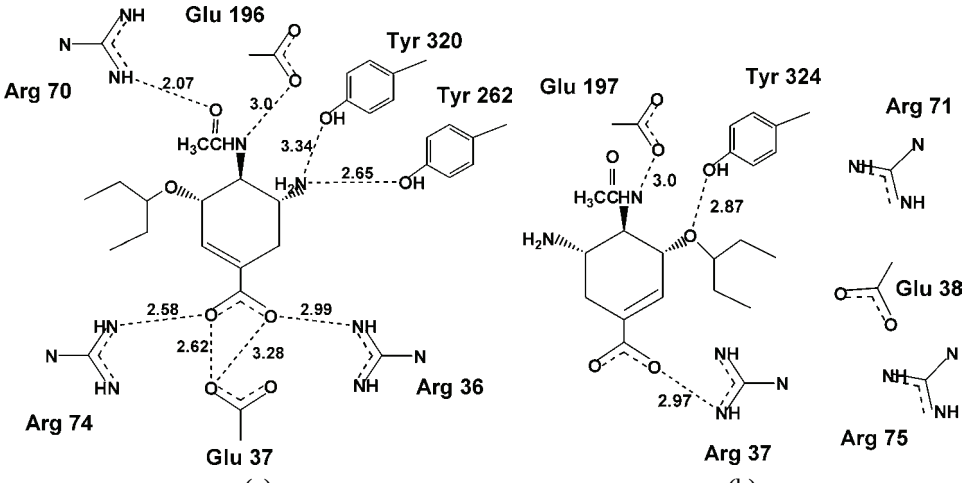

Fig. 4. The binding interactions (in Å) of oseltamivir with the residues in the active site of H5N1-NA (a) and N9-NA (b).

N9–NA binding site on OTV is quite clear. This is in agreement with the binding free energies, –6.63 and –7.47 kcal mol^{-1}, of OTV docked into N9-NA and H5N1-NA, respectively (Table I). A slight difference of less than 1 kcal mol^{-1} between the binding free energies of OTV-N9 and OTV-N1 is in agreement with the experimentally predicted free energy difference[23] but significantly in contrast to the computationally predicted lower susceptibility of OTV to N1 than to N9 by about 6 kcal mol^{-1}.[7] Also, there are no differences between the net charges of the OTV side chains in the complexes with H5N1-NA and N9-NA, as given in Table I.

TABLE I. The binding free energies and the AM1 net charges of the side chains of various ligands in the complexes

Model	Ligand	$\Delta G_{binding}$ kcal mol^{-1}	Charge (e)		
			Amide/–OH side chain	–NH side chain	Glycerol/ether/alkyl side chain
H5N1-NA	Zanamivir	–6.80	+1	–17	–23
	Oseltamivir	–7.47	–6	–17	–33
	DANA	–7.49	–3	–15	–7
	Peramivir	–7.82	–18	–15	–36
N9-NA	Zanamivir	–6.51	–19	–17	–21
	Oseltamivir	–6.63	–6	–17	–33
	Peramivir	–7.23	–10	–17	–34
	DANA	–7.97	–3	–17	–25

Comparison of the efficacies of ZMV, OTV and PMV against N1 and N9 NAs was previously reported in the literature.[23] The ranges of experimental IC_{50} (nm) values for N1-NA were 5.8–19.7 for ZMV, 36.1–53.2 for OTV and 2.6–3.4 for PMV, while those for N9-NA were 10.4–11.5 for ZMV, 9.5–17.7 for OTV and 0.9–1.6 for PMV.[23] The trend of the experimental IC_{50} values for N9-NA is in agreement with that of the calculated binding free energies (Table I). In contrast, the trend of the experimental IC_{50} values for ZMV and OTV bound to N1-NA slightly deviates from that of the binding free energies (Table I).

The –NHAc group of OTV makes only one polar contact with Glu197 in N9-NA, while it makes two polar contacts with Arg70 and Glu196 in H5N1-NA (Fig. 4). By focusing on the positions of the –O–R and $–NH_2$ side chains of OTV in N9-NA with respect to those in H5N1-NA, OTV docked into N9-NA is rotated by 180° relative to that docked into H5N1-NA, thus enabling the $–NH_2$ group to make two electrostatic interactions with Tyr262 and Tyr320 in H5N1-NA (Fig. 4). By noting the particular locations of Arg74, Arg70, and Glu37 in H5N1-NA relative to those of Arg75, Arg71, and Glu38 in N9-NA (Fig. 4), the OTV flip in H5N1-NA relative to N9-NA is also associated with active-site amino-acid reorientation. While the –O–R group of OTV makes an electrostatic interaction with Tyr324 in N9-NA, it does not make any contact with the active-site residues in H5N1-NA. Since the –O–R group of OTV is capable of rotating around the single bond

between the oxygen and alkyl chain R, it inclines to adapt itself and take a comfortable position relative to its environment. In this context, noteworthy is the structure of OTV docked into the active site of H5N1-NA (Fig. 5) and N9-NA (Fig. 6), respectively. A pocket containing residues Arg144, Glu197, and Ala166 is present in the complex of N9-NA, while the pocket is spoiled in the complex of H5N1-NA.

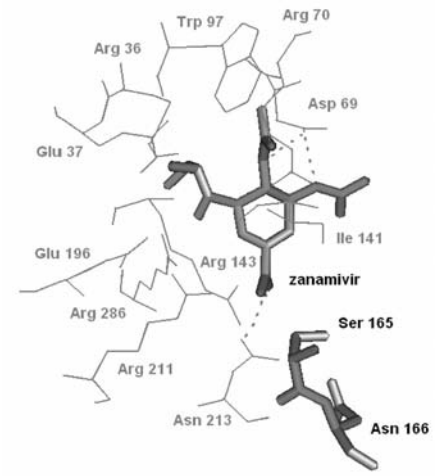

(a)

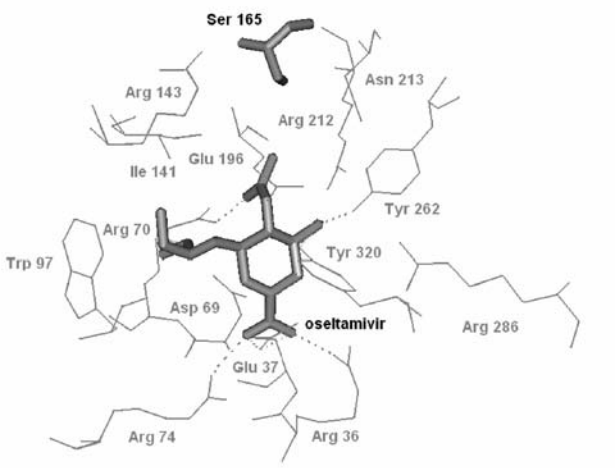

(b)

Fig. 5. The structures of zanamivir (a) and oseltamivir (b) docked into the active site of H5N1-NA.

In the case of OTV, which has been much more widely used than ZMV, a viable resistant influenza virus mutant has emerged.[24] This oseltamivir resistant virus remains sensitive to zanamivir, a drug derived from the naturally occurring sialic acid Neu5Ac with negligible additional functionalization.[24] ZMV can also

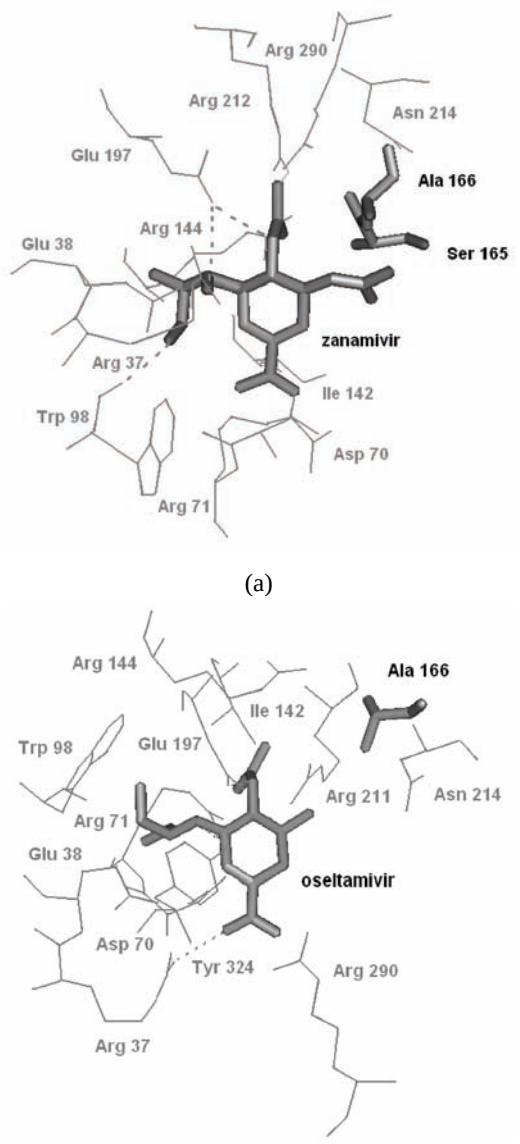

Fig. 6. The structures of zanamivir (a) and oseltamivir (b) docked into the active site of N9-NA.

be viewed as an inhibitor derived from DANA,[11] in which a hydroxyl group on C4 is substituted by a guanidino group (Fig. 1). The binding of ZMV and DANA to either H5N1-NA or N9-NA was considered to be very comparable in terms of electrostatic interactions made with the NA active sites.[6] By having a five-membered instead of a six-membered ring, peramivir is structurally different from ZMV, DANA and OTV (Fig. 1). For all these reasons, it is interesting to quantitatively compare the binding of the four inhibitors to H5N1-NA and N9-NA (Table I).

The binding free energies of ZMV, OTV, DANA, and PMV docked into H5N1-NA are –6.80, –7.47, –7.49 and –7.82 kcal mol^{-1}, respectively. The binding free energies of ZMV, OTV, PMV, and DANA docked into N9-NA are –6.51, –6.63, –7.23 and –7.97 kcal mol^{-1}, respectively. Note that all the inhibitor/H5N1-NA or N9-NA binding free energies are similar to each other, *i.e.*, within 1.00 or 1.45 kcal mol^{-1}. Two previous observations,[5] based on a computational model of H5N1-NA, that N1–ligand binding is less potent than N9–ligand binding and that the binding free energies of the zanamivir–N1/N9 complexes are lower than those of the oseltamivir–N1/N9 complexes, do not seem to hold fast herein (Table I). The charge distribution was evaluated using the semi-empirical AM1 method. The total net charges of the –NH side chain of ZMV, OTV, and DANA are almost equal (–17 e) in all the complexes. The total net charges, –23 and –21 e, of the glycerol side chain of ZMV in the ZMV–N1/N9 complexes are less negative than those of the ether side chain of OTV in the OTV–N1/N9 complexes (–33 e). It is interesting to observe that the total net charge (–6 e) of the amide side chain of OTV in OTV–N1 is more negative than that (+1 e) of ZMV in ZMV–N1. In contrast to this, the total net charge (–6 e) of the amide side chain of OTV in OTV–N9 is less negative than that (–19 e) of ZMV in ZMV–N9. These trends of the AM1 charges of the ZMV and OTV side chains in the complexes disagree with those previously reported in the literature.[5] The present analysis indicates that a major difference between ZMV/OTV bound to either H5N1-NA or N9-NA is reflected through the net charges of their glycerol/ether and amide/amide side chains. In addition, Table I indicates that a main difference between ZMV bound to H5N1-NA and ZMV bound to N9-NA is reflected through the net charges of the amide side chains of ZMV. This might indicate that potential modifications of the ZMV amide side chain could lead towards the design of novel NA inhibitors with a strong resemblance to the natural substrate sialic acid. Since the oseltamivir resistant virus remains sensitive to zanamivir,[1,24] maintaining a strong resemblance to the natural substrate might reduce the possibility of developing viable drug-resistant mutants.

An interesting question to be elucidated is: how does the previously established, subtle variation between lipophilic and hydrophilic environments in H5N1-NA with respect to N9-NA influence the binding of ZMV and OTV to H5N1-NA and N9-NA? As shown in Fig. 3, the lipophilic Ala261 and Tyr262 (hydrophilic Ser165 and Asn166) in H5N1-NA complexed with OTV correspond to the hydrophilic Asn265 and Asn266 (lipophilic Ala166 and Thr167) in N9-NA complexed with OTV. Thus, the structures of zanamivir and oseltamivir docked into the active sites of H5N1-NA and N9-NA are shown in Figs. 5 and 6, respect–tively. Note the presence of Ser165 and Asn166 in the H5N1-NA active site of ZMV, while only Ser165 is present in the H5N1-NA active site of OTV. By focusing on the particular positions of Ser165 (Fig. 5), a clear reorientation of the

H5N1–NA active site residues of OTV relative to those of ZMV may be ascribed to both the presence/absence of Asn166 in the active cavity of ZMV/OTV and the –O–R side chain of OTV, which is able to rotate around the single O–R bond. Note also the presence of Ser165 and Ala166 in the N9-NA active site of ZMV, while only Ala166 is present in the N9-NA active site of OTV. By focusing on the particular positions of Ala166 (Fig. 6), a clear reorientation of the N9-NA active site residues of OTV relative to those of ZMV may be ascribed to both: the presence/absence of Ser165 in the active cavity of ZMV/OTV and the –O–R side chain of OTV, that is able to rotate around its single O–R bond.

CONCLUSION

Neuraminidases (NA) homology models of good stereochemical quality have been shown to be a valuable means of revealing the secret associated with the high resistance of some H5N1 strains to the commercial drugs ZMV and OTV. Thus, subtle conformational differences underlying the binding of ZMV and OTV to either H5N1-NA or N9-NA were detected. The conformational differrences were shown to be more quantitatively reflected through the side chain charges of ZMV and OTV than through the binding free energies of their complexes. In this way, the previous experience that an oselatmivir-resistant virus remains sensitive to zanamivir, a drug derived from the naturally occurring sialic acid Neu5Ac with slight functional modifications, was addressed. This might provide a more profound impact on reducing the possibility of developing viable drug-resistant mutants.

SUPPLEMENT

Supplementary material (PDB files of the H5N1-NA and N9-NA structural models) is available upon request to authors.

Acknowledgment. This work was supported by Grant No. 143016B from the Ministry of Science and Technological Development of the Republic of Serbia.

И З В О Д

НОВИ УВИДИ У МЕХАНИЗМЕ ВЕЗИВАЊА ОСЕЛТАМИВИРА И ЗАНАМИВИРА СА НЕУРАМИНИДАЗАМА H5N1 И N9 ВИРУСА ГРИПА: СТУДИЈА НА БАЗИ ХОМОЛОГНОГ МОДЕЛИРАЊА И МОЛЕКУЛАРНОГ ДОКИНГА

МАРИЈА Л. МИХАЈЛОВИЋ[1,2] и ПЕТАР М. МИТРАШИНОВИЋ[2]

[1]*Факултет за физичку хемију, Универзитет у Београду, Студентски трг 12–16, 11000 Београд и* [2]*Институт за мултидисциплинарна истраживања, Кнеза Вишеслава 1, 11030 Београд*

У контексту недавне опасности од ширења вируса птичијег грипа H5N1, нови увиди у механизме везивања различитих инхибитора (занамивир-ZMV, оселтамивир-OTV, DANA, перамивир-PMV) са неураминидазама (NA) су од виталне важности за структурно дизајнирање нових антивирусних лекова. Да би се обезбедили ови увиди, тродимензионални модели неураминидаза H5N1 и N9 су генерисани путем хомологног моделовања. Традиционалне аминокиселине које су присутне у везивним местима целе фамилије неураминидаза су такође конзервисане у H5N1. Установљена је суптилна варијација липофилног и хидрофилног

окружења у H5N1 у поређењу са N9, чиме се даје допринос даљем разјашњењу високе резистенције вируса H5N1 на инхибиторе неураминидаза. На бази хомологних модела урађен је флексибилан докинг применом ArgusLab4/ASkor протокола. Конформационе разлике између OTV везаног за H5N1-NA и везаног за N9-NA су структурно идентификоване и квантификоване. Разлика у везивној слободној енергији, која је мања од 1 kcal mol^{-1} за OTV–H5N1/N9-NA комплексе, у сагласности је са експерименталном вредности из литературе. Такође конформационе разлике између ZMV и OTV везаних за H5N1-NA и N9-NA су идентификоване. Везивне слободне енергије за занамивирове комплексе које су незнатно више у односу на вреднсти за оселтамивирове комплексе нису у сагласности са претходним вредностима из литературе које су базиране на хомологном моделовању. Предложено је да се ове разлике између ZMV и OTV могу објаснити присуством/одсуством аминокиселине Asn166 у везивном месту ZMV/OTV са H5N1-NA, као и присуством/одсуством аминокиселине Ser165 у везивном месту ZMV/OTV са N9-NA. Дистрибуција наелектрисања је процењена применом полуемпиријског AM1 метода. Трендови наелектрисања бочних ланаца занамивира и оселтамивира у комплексима се разликују од претходно објављених трендова.

(Примљено 2. априла, ревидирано 21. октобра 2008)

REFERENCES

1. M. Von Itzstein, *Nature Reviews Drug Discovery* **6** (2007) 967
2. R. J. Russell, L. F. Haire, D. J. Stevens, P. J. Collins, Y. P. Lin, G. M. Blackburn, A. J. Hay, S. J. Gamblin, J. J. Skehel, *Nature* **443** (2006) 45
3. Y. Liu, J. Zhang, W. Xu, *Current Med. Chem.* **14** (2007) 2872
4. C. Sangma, S. Hannongbua, *Current Computer-Aided Drug Design* **3** (2007) 113
5. P. Nimmanpipug, J. Jitonnom, C. Ngaojampa, S. Hannongbua, V. S. Lee, *Molec. Simul.* **33** (2007) 487
6. D.-Q. Wei, Q.-S. Du, H. Sun, K.-C. Chou, *Biochem. Biophys. Res. Commun.* **344** (2006) 1048
7. O. Aruksakunwong, M. Malaisree, P. Decha, P. Sompornpisut, V. Parasuk, S. Pianwanit, S. Hannongbua, *Biophys. J.* **92** (2007) 798
8. M. Mase, K. Tsukamoto, T. Imada, K. Imai, N. Tanimura, K. Nakamura, Y. Yamamoto, T. Hitomi, T. Kira, T. Nakai, M. Kiso, T. Horimoto, Y. Kawaoka, S. Yamaguchi, *Virology* **332** (2005) 167
9. G. M. Air, R. G. Webster, P. M. Colman, W. G. Laver, *Virology* **160** (1987) 346
10. (a) N. Guex, M. C. Peitsch, *Electrophoresis* **18** (1997) 2714; (b) T. Schwede, J. Kopp, N. Guex, M. C. Peitsch, *Nucleic Acids Res.* **31** (2003) 3381; (c) N. Guex, A. Diemand, T. Schwede, M. C. Peitsch, *Swiss-Model 3.5: An Automated Comparative Protein Modeling Server*, http://www.expasy.org/swissmod/SWISS-MODEL.html (2008)
11. B. J. Smith, P. M. Colman, M. Von Itzstein, B. Danylec, J. N. Varghese, *Protein Sci.* **10** (2001) 689
12. J. W. Ponder, *Tinker Molecular Modeling Package*, http://dasher.wustl.edu/tinker (2004)
13. J. W. Ponder, *Force Field Explorer 4.2: A Graphical User Interface to Tinker*, http:// //dasher.wustl.edu/tinker (2004)
14. J. Wang, P. Cieplak, P. A. Kollman, *J. Comput. Chem.* **21** (2000) 1049
15. R. A. Laskowski, M. W. MacArthur, D. S. Moss, J. M. Thornton, *J. Appl. Cryst.* **26** (1993) 283
16. A. L. Morris, M. W. MacArthur, E. G. Hutchinson, J. M. Thornton, *Proteins* **12** (1992) 345
17. W. L. DeLano, *PyMol*^{TM} *0.97*, DeLano Scientific LLC, San Carlos, CA, 2004.

18. M. A. Thompson, *ArgusLab 4.0*, Planaria Software LLC, Seatle, NY, 2004.
19. W. J. Brouillette, S. N. Bajpai, S. M. Ali, S. E. Velu, V. R. Atigadda, B. S. Lommer, J. B. Finley, M. Luo, G. M. Air, *Bioorg. Med. Chem.* **11** (2003) 2739
20. C. U. Kim, W. Lew, M. A. Williams, H. Wu, L. Zhang, X. Chen, P. A. Escarpe, D. B. Mendel, W. G. Laver, R. C. Stevens, *J. Med. Chem.* **41** (1998) 2451
21. T. Wang, R. C. Wade, *J. Med. Chem.* **44** (2001) 961
22. A. R. Ortiz, M. T. Pisabarro, F. Gago, R. C. Wade, *J. Med. Chem.* **38** (1995) 2681
23. E. A. Govorkova, I. A. Leneva, O. G. Goloubeva, K. Bush, R. G. Webster, *Antimicrob. Agents Chemother.* **45** (2001) 2723
24. Q. M. Le, M. Kiso, K. Someya, Y. T. Sakai, T. H. Nguyen, K. H. L. Nguyen, N. D. Pham, H. H. Ngyen, S. Yamada, Y. Muramoto, T. Horimoto, A. Takada, H. Goto, T. Suzuki, Y. Suzuki, Y. Kawaoka, *Nature* **437** (2005) 1108.